IIIII ISS Electrostatic Levitation Furnace, ELF IIIII
(Review)

Numerical Estimation of Convection in a Molten Zirconium Droplet Processed by Electromagnetic Levitation in Microgravity

Jonghyun LEE [1] and Robert W. HYERS[2]

Abstract

As a part of ground support activities for the upcoming experiments in the International Space Station (ISS), convection inside a molten Zr, one of flight samples was numerically predicted. The sample will be processed with the materials science laboratory – electromagnetic levitation (MSL-EML) facility which has already been installed in the European deck. Thermophysical properties, such as, heat capacity, thermal conductivity, viscosity and surface tension of the molten Zr will be measured. The validity of some of these properties are significantly affected by convection during the measurements and the convection must be predicted in advance to help design the space experiments. Utilizing the magnetohydrodynamic (MHD) model developed in the previous research, a series of simulations was performed in order to investigate the convection during the space experiments.

Keyword(s): Magnetohydrodynamic Modeling, Convection, Electromagnetic Levitation, Zirconium, Microgravity

Received 24 Oct. 2014, accepted 16 Jan. 2015, published 31 Jan. 2015

1. Introduction

Acquiring accurate thermophysical properties of industrially important metals benefits both industry and science. Density, viscosity, surface tension, heat capacity, and thermal conductivity are the essential properties needed for understanding and controlling of various kinds of liquid metals processing, such as casting. An accurate measurement of these properties at high temperatures is a challenging task due to high reactivity. Containerless processing can be an effective way of dealing with highly reactive liquid materials at high temperatures. During last decades, several containerless processing methods have been developed and utilized to measure thermophysical properties of molten metals and ceramics. One of widely applied methods is electromagnetic levitation (EML). EML utilizes an electromagnetic (EM) field to levitate and to heat a conductive sample simultaneously. On the ground, the minimum strength of an EM field to counteract gravity is large enough to induce a significant amount of stirring in a molten metal. Therefore, with ground-based EML, we always have a turbulent flow which affects some thermophysical properties measured by EML. In order to overcome this negative effect of gravity, a series of experiments will be performed in ISS by early 2015. Using MSL-EML, thermophysical properties mentioned above will be measured. In microgravity, one can induce a much wider range of convection in a molten sample, i.e., from laminar to turbulent regimes. For an effective and efficient design of space experiments, the convection in the sample must be predicted with a reasonable level of accuracy. This research predicts the convection in one of flight samples, Zr, using the MHD model developed and experimentally validated in the previous research [1)]. The simulation results will inform the amount of convection as a function of processing parameters during the space experiments.

2. Property Measurement using EML

2.1 EML

A conductive sample sized 5-8 mm in diameter can be levitated and processed using EML. EML employs a set of coils wound with copper tubes which generates an EM force field around the sample. Excessive heating of the copper tubes is prevented by water coolant. The coil consists of two parts: upper and lower coils. For the ground-based EML which typically induces one electric current through one set of coil to levitate and heat up the sample simultaneously, the upper and lower coils must be wound in the opposite direction to each other. The lower coil creates an EM force field upward to cancel the weight of the sample, meanwhile the upper coil downward to press down the sample securing the stability during processing. The mass of EML samples is around 1 g. On earth, a minimum EM force needed for stable levitation of the sample is large enough to induce a turbulent flow. The turbulence in the molten sample is beneficial for the measurement of heat capacity in that it provides much higher convective heat transfer within the sample and reduces time to

1 Department of Mechanical and Industrial Engineering, Research Assistant Professor, University of Massachusetts, 160 Governors Drive, Amherst, MA 01002, USA.
2 Department of Mechanical and Industrial Engineering, Professor, University of Massachusetts, 160 Governors Drive, Amherst, MA 01002, USA.
(E-mail: jonghyunlee@ecs.umass.edu)

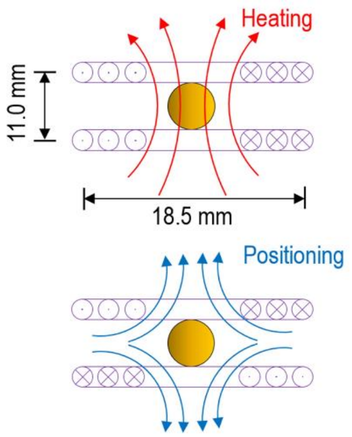

Fig. 1 SUPOS coil set used in MSL-EML [4)]

reach thermal equilibrium. However, for other properties such as viscosity, surface tension, and thermal conductivity, the presence of turbulence must be avoided at all costs.

Acceleration inside ISS is less than gravity on Earth by an order of 10^{-4}. In such a microgravity condition, the minimum amount of current to stabilize a sample is reduced drastically and the range of accessible convection becomes much wider. For instance, the Reynolds number (Re) for a molten 7 mm $Fe_{50}Co_{50}$ sample in ground-based EML is 2800 whereas in space the Re ranges from 40 to 1400 [2)]. Considering that the Reynolds number near the laminar to turbulent transition is around 600 [3)], it can be known that one can access both the laminar and turbulent regimes using space EML.

MSL-EML is equipped with one set of coil, called SUPOS which stands for superposition, as shown in **Fig. 1**. Through this coil set, alternating currents for both heating and positioning purposes run at 350 kHz and 150 kHz respectively. The directions of heating currents in both the upper and lower coils are the same such that a dipole EM field is generated (upper figure). This dipole field is efficient in heating a sample. Meanwhile, the positioning currents create a quadrupole EM field to stabilize a sample near the center of the coil set.

During operation, an astronaut will control the coil current by adjusting voltage nobs on the control panel. This control voltage varies from 0 to 10 V. The heating and positioning currents are proportional to the control voltages as shown in Equation (1).

$$I_H = 19.09 + 19.09 \cdot V_H^{Ctrl}$$
$$I_P = 27.21 + 27.21 \cdot V_P^{Ctrl} \qquad (1)$$

where I_H is the heating current, I_P is the positioning current in A, V_H^{Ctrl} is the heater control voltage, and V_P^{Ctrl} is the positioner control voltage in V. The maximum heating and positioning currents happen when the control voltage is set at 10 V and the values are 209.99 A and 299.31 A respectively. The minimum currents are set to be above zero even without control voltage in order to keep the system in the 'warmed-up' condition. The size of samples for the MSL-EML also has a range of 5-8 mm.

2.2 Viscosity and Surface Tension

The viscosity and surface tension are measured by a method called the oscillating droplet technique. A levitated sample is excited by a modulating EM field at a frequency near the natural frequency of the sample. After obtaining adequate excitation, the modulating EM field is removed and the sample begins to dampen freely. The dampening motion of the sample is captured with a high-speed camera and the captured images are analyzed to extract the decay time and the oscillation frequency, from which the viscosity and surface tension can be estimated by the relationships given in Equation (2) [5)].

$$\mu = \frac{\rho R_o^2}{(l-1)(2l+1)\tau}$$
$$\gamma = \frac{3\pi m f^2}{l(l-1)(l+2)} \qquad (2)$$

where μ is the viscosity, ρ is the density, R_o is the initial radius of a sample, l is the mode number which is 2 in this case, τ is the damping constant, γ is surface tension, f is the oscillation frequency of a sample in cycles per second.

In order to measure the molecular viscosity, the main mechanism of damping must be intermolecular friction. If the turbulence presents in the sample, the measured viscosity should become much higher due to the effect of turbulent eddy dissipation. Our prediction showed that the effective turbulent viscosity of a molten $Cu_{84}Co_{16}$ sample was about 50 times higher than its molecular viscosity at the estimated Reynolds number of 2400 [1)]. For the viscosity measurement using the oscillating droplet technique, it is of critical importance to know the convection status, i.e., either laminar or turbulent, under given combinations of test parameters.

2.3 Heat Capacity and Thermal Conductivity

The modulation calorimetry is a method of measuring heat capacity and thermal conductivity for both solids and liquids. When applied in EML [6)-8)], a heating EM field is modulated to heat up the sample. In an EML sample, most of the eddy current happens near the surface, called skin depth (δ) defined as

$$\delta = \sqrt{\frac{2}{\mu_m \omega \sigma_e}} \qquad (3)$$

with μ_m and σ_e being the magnetic permeability and the electrical conductivity respectively. ω is the modulation frequency which is to be small enough to allow much faster internal thermal relaxation of the sample than the period of modulation. Due to resistance of the sample, heat is generated in the skin depth near the side surface and transferred to the middle and top part of the sample. By measuring the time lag between the modulation current and the temperature response measured from the top portion of the sample, the thermal conductivity can be estimated. Possible mechanisms of heat transfer are conduction, convection, and radiation. For a solid sample, convection is ruled out. If the temperature is not very high, radiation can also be neglected. Meanwhile, a great care must be taken for the case of a liquid sample. Either the EM force or the temperature gradient induces convection inside the sample. As the convection increases, the convective heat transfer becomes dominant and the measured thermal conductivity becomes invalid. Therefore, the status of convection in the EML sample must be ensured to be in an extreme laminar regime, when the thermal conductivity is measured.

3. Governing Equations and Modeling

3.1 Governing Equations for Fluid Flow

Fluid flow in molten metals can be assumed to be viscous and incompressible, and it is governed by the Navier-Stokes Equations.

$$\begin{gathered}\nabla^* \cdot \vec{u}^* = 0 \\ \frac{\partial \vec{u}^*}{\partial t^*} + \vec{u}^* \cdot \nabla^* \vec{u}^* = -\nabla^* P^* + \frac{1}{Re}\nabla^{*2}\vec{u}^* + \vec{F}^*\end{gathered} \tag{4}$$

where $\vec{u}^*$ is the velocity, P^* is the pressure, and $\vec{F}^*$ is the body force in a dimensionless form. $\vec{F}^*$ is the EM force for the case of an EML sample. It can be noticed that the flow is characterized by a single dimensionless number, the Reynolds number, which defines the ratio of inertial effects to viscous effects.

$$Re = \frac{\rho U D}{\mu} \tag{5}$$

where ρ is the density, U is the velocity, D is the diameter of a droplet, and μ is the molecular viscosity. No flow across and no shear stress on the surface of a droplet were assumed as described in Equation (6).

$$\vec{u}^* \cdot \vec{\iota}_r |_{r^*=1} = \vec{\tau}^* \cdot \vec{\iota}_t |_{r^*=1} = 0 \tag{6}$$

where, $\vec{\iota}_r$ and $\vec{\iota}_t$ are the unit vectors in the radial and tangential directions respectively.

For turbulence, the renormalization group (RNG) k-ε model was adopted. The RNG k-ε model adds two more equations on the turbulent kinetic energy (k) and the turbulent dissipation (ε) in order to deal with the Reynolds stress term introduced by the random nature of turbulence. The RNG k-ε model has been proven to be suitable for swirling flows, stagnation flows, and low Reynolds number and transitional flows [9]. No gradient in the radial direction on the boundaries was assumed for k and ε as written in Equation (7)

$$\left.\frac{\partial k^*}{\partial r^*}\right|_{r^*=1} = \left.\frac{\partial \varepsilon^*}{\partial r^*}\right|_{r^*=1} = 0 \tag{7}$$

3.2 Electromagnetic Force

An EM force field generated in the volume of an EML droplet was obtained by numerically solving the Maxwell's equations with parameters such as the geometry of the sample and coil, the electrical conductivity of the sample, and the positioning/heating currents and frequencies. The EML system can be regarded as magnetoquasistatic and the Maxwell's equations can be simplified as in Equation (8) [1].

$$\begin{gathered}\nabla \times \vec{B} = 0 \\ \nabla \times \vec{E} = -\frac{\partial \vec{B}}{\partial t} \\ \nabla \times \vec{H} = \vec{J}\end{gathered} \tag{8}$$

where $\vec{B}$ is the magnetic flux density, $\vec{E}$ is the electric field, $\vec{H}$ is the magnetic field, and $\vec{J}$ is the current density. The system of differential equations was solved using an appropriate numerical technique and the resulting distribution of EM forces in the sample was implemented into the numerical model using a user-defined subroutine.

3.3 Numerical Modeling

The MHD model which had been developed using ANSYS Fluent™ and experimentally validated in the previous research [1] was used for the current study. In this model, the flow was assumed to be axisymmetric and the flow domain was modeled with a half circle with the diameter of 6.71 mm. The density (ρ), the viscosity (μ), and the electrical conductivity (σ) of Zr used for the simulation are listed in **Table 1**. The melting point of Zr is 2128 K. More details on the numerical modeling can be found elsewhere [1)-4)].

4. Results and Discussion

The Zr sample included in the first batch for the ISS experiments is to be used for the calibration of cameras and to serve as a reference sample for some thermophysical properties, such as density and heat capacity both in solid and in liquid

Table 1 Material properties of Zr

Properties	Temperature Dependence
ρ (kg·m^{-3})	$6240 - 0.29(T - T_m)$
μ (mPa·s)	$4.74 - 4.97 \times 10^{-3}(T - T_m)$
σ (Ω^{-1}·m^{-1})	6.79×10^5

states, and surface tension and viscosity. The status and magnitude of convection were predicted under possible combinations of positioner, heater control voltage, and temperature. Based on the predicted results, allowable combinations of test parameters are to be determined for the viscosity and thermal conductivity measurements.

4.1 Convection Velocity

A series of simulations was performed with the increasing heater control voltage (0 – 10 V) while the positioner voltage being fixed at 8 V. The predicted maximum convection velocities and the corresponding Reynolds number were plotted at various temperatures in **Fig. 2**. It was assumed that the sample would be superheated up to 300 K above and undercooled down to 400 K below the melting point. The maximum convection velocity and the corresponding Reynolds number were plotted only up to the heater control voltage of 4 V to show more details in the region of lower heater control voltage. For the measurements of viscosity and thermal conductivity, the convection must be minimized and any small amount of turbulence in the sample must be avoided. Therefore, it is reasonable to use the maximum convection velocity for the estimation of the Reynolds number to judge the status of the flow conservatively. The laminar to turbulent transition was assumed to occur near the Reynolds number of 600 [3]. The laminar model was applied until the Reynolds number reached 600 and the turbulent model was used thereafter.

From the left plot in **Fig. 2**, it can be noticed that in the laminar regime, the maximum convection velocity decreases up to around the heater control voltage of 1 V and then it starts to increase as the heater control voltage is added up. This is because the direction of EM forces generated by the positioner current are opposite to that by the heater current in some region of the sample. After 1 V of the heater control voltage, the EM field becomes heater-dominant and the convection velocity increases monotonically. In the turbulent regime, the maximum convection velocity increases almost linearly with an increase of the heater control voltage. At 10 V of the heater control voltage, the maximum convection velocity reaches 0.49 $m \cdot s^{-1}$. Higher temperature yields larger convection as the viscosity drops down. Under a given range of temperature (1728 – 2428 K), the influence of temperature on the maximum convection velocity is less than 9 % and 1% in the laminar and turbulent regimes, respectively. These differences are smaller compared to the case of the $Fe_{50}Co_{50}$ sample [4]. The smaller temperature dependence for Zr could be attributed to the fact that the temperature dependence of the density and viscosity of $Fe_{50}Co_{50}$ is larger than that of Zr over the simulated temperature range.

From the Reynolds number plot, it can be noticed that at Tm+300 K, the flow becomes transitional even with no heater control voltage. It implies that the positioner current alone does affect the status of the flow at high temperatures and that at Tm+300 K with the positioner control voltage of 8 V, the measurement of viscosity or thermal conductivity must not be made. Since the viscosity drops at a rate faster than density with an increasing temperature, the Reynolds number becomes

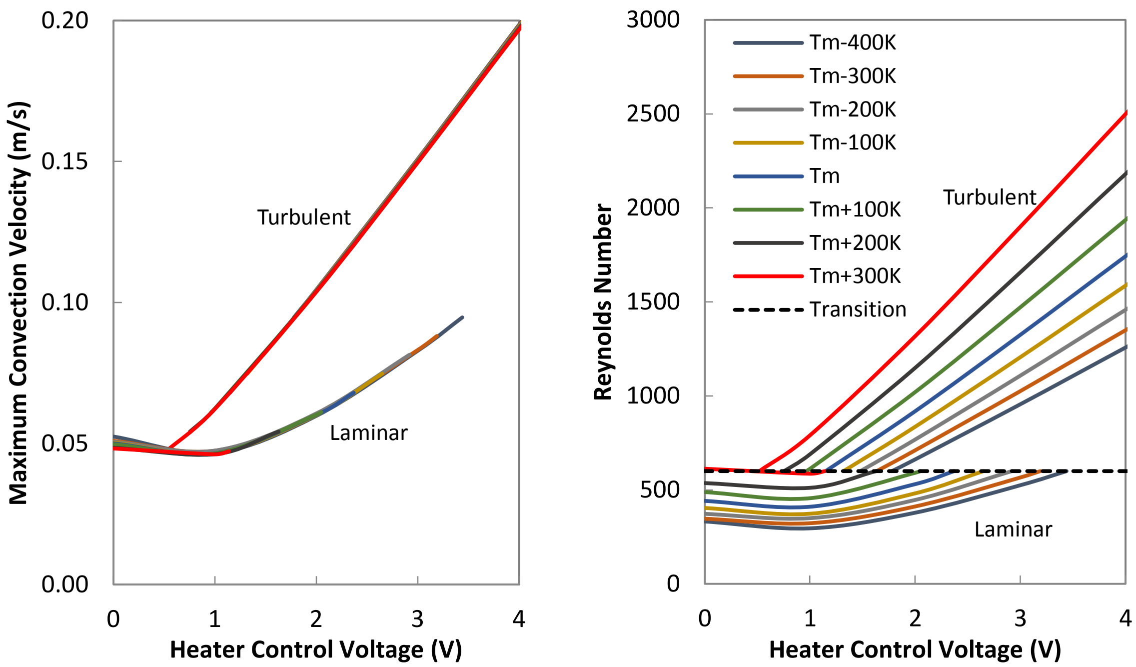

Fig. 2 Maximum convection velocity developed inside a molten Zr sample of 6.71 mm in diameter as a function of the heater control voltage and temperature. The positioner control voltage was fixed at 8 V for all cases.

Tm – 300 K

Positioner ctrl V [V] \ Heater ctrl V [V]	0	0.2	0.4	0.6
6	361	413	490	582
7	395	427	500	576
8	421	449	511	577
9	451	476	532	598
10	487	506	555	622

Tm – 200 K

Positioner ctrl V [V] \ Heater ctrl V [V]	0	0.2	0.4	0.6
6	390	447	530	630
7	427	462	541	624
8	456	486	553	624
9	487	515	576	647
10	527	548	601	673

Tm – 100 K

Positioner ctrl V [V] \ Heater ctrl V [V]	0	0.2	0.4	0.6
6	425	487	578	686
7	466	503	590	680
8	496	530	603	680
9	531	561	627	705
10	574	597	654	734

Tm

Positioner ctrl V [V] \ Heater ctrl V [V]	0	0.2	0.4	0.6
6	468	535	635	755
7	512	553	649	747
8	546	583	663	748
9	584	617	690	775
10	632	656	720	807

Tm + 100 K

Positioner ctrl V [V] \ Heater ctrl V [V]	0	0.2	0.4	0.6
6	520	595	706	839
7	569	615	721	831
8	607	648	737	832
9	650	686	767	862
10	702	730	800	897

Tm + 200 K

Positioner ctrl V [V] \ Heater ctrl V [V]	0	0.2	0.4	0.6
6	587	671	796	946
7	642	694	813	937
8	684	730	831	938
9	732	773	865	972
10	792	823	902	1011

Laminar (Re < 500) Transition (500 < Re < 700) Turbulent (Re > 700)

Fig. 3 Distribution of the Reynolds number as a function of the positioner and heater control voltages.

larger even with the similar convection velocities. The Reynolds number with 10 V of the heater control voltage at Tm+300 K is around 6200. As is in the case of the convection velocity, the Reynolds number in the laminar regime first decreases and increases before and after 1 V of the heater control voltage and increases in the turbulent regime almost linearly.

In order to examine the influence of positioner current on the convection status, more simulations were performed with the varying positioner control voltage (6 – 10 V) and the smaller heater control voltage (0 – 0.6 V). The Reynolds number for each case was estimated again with the maximum convection velocity and tabulated in **Fig. 3**. Assuming that the laminar to turbulent transition occurs over the range of Reynolds number from 500 to 700, the cells were colored in white (laminar), orange (transition), and red (turbulent) based on the flow status. At undercooled temperatures, the flow remains mostly either in the laminar or transition regime over the range of the positioner control voltage considered due to the increased viscosity. In contrast, no laminar flow can be obtained at superheated temperatures.

4.2 Application to Viscosity Measurements

Figure 4 shows a typical temperature-time plot for the viscosity measurement. A solid sample is heated until it is melted and superheated up to a desired temperature. Both the positioner and heater control voltages were set at high enough values up to the maximum superheated temperature. As depicted in **Fig. 1**, the heating current exerts an upward and downward resultant force to the sample. High heater current may jeopardize the stability of the sample. Therefore, if the heater control voltage increases, the positioner control voltage must be also increased to secure the stability of the sample. In the opposite case, if the heater control voltage decreases, the positioner control voltage can be reduced. In **Fig. 4**, the positioner control voltage is also decreased to reduce convection

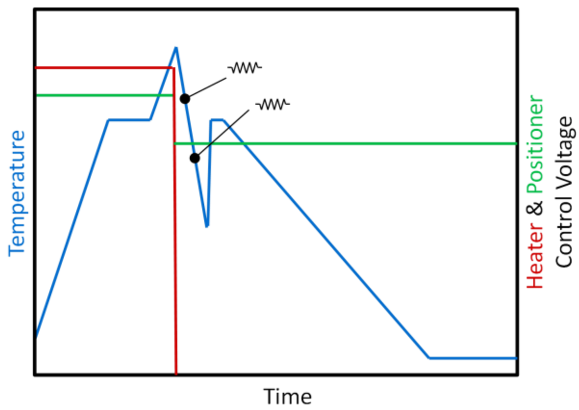

Fig. 4 Temperature-time plot for viscosity measurement.

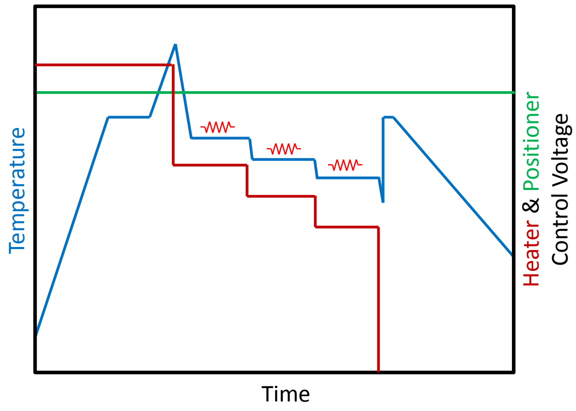

Fig. 5 Temperature-time plot for modulation calorimetry.

in the sample as the heater control voltage is turned off at the maximum temperature. As soon as the heater control voltage is turned off, the sample begins to cool down. During this cooling stage, the sample is oscillated by adding a small amount of heater current alternating at the frequency near the natural frequency of the sample. Depending on the degree of undercooling, a few oscillations can be induced – some possibly in the superheated region and some possibly in the undercooled region. With the positioner control voltage of 6 – 10 V, there will be a high probability of having turbulence even without heater control voltage. It means that the viscosity data at superheated temperatures must be measured with the positioning control voltage less than 6 V. The influence of the positioner current on convection is not negligible such that even for the undercooled region, it is safer to set the positioner control voltage as low as possible to avoid turbulence.

4.3 Application to Thermal Conductivity and Heat Capacity Measurements

A typical thermal profile for the modulation calorimetry is shown in **Fig. 5**. After reaching the maximum temperature, only the heater control voltage was lowered to a certain amount and held to reduce the sample temperature down to the desired equilibrium temperature. For each thermal hold, the modulation calorimetry is performed to measure the heat capacity and thermal conductivity of the sample. The range of planned thermal hold temperature is from 1923 K to 2193 K. Our calculation showed that the required heater control voltages are 6.9 V and 8.7 V for the lower and upper equilibrium temperatures, respectively. With such high heater control voltages, the EM force field becomes heater-dominent and the influence of the positioning control voltage on the convection velocity becomes negligible (0.3 % with a span of 6 to 10 V). The estimated Reynolds numbers for the lower and upper ends are 2550 and 4330 repectively, which implies that under the desired range of temperature, the flow will be turbulent. With turbulence, the heat capacity can be measured effectively due to the enhanced heat transfer by turbulent mixing, whereas, the thermal conductivity cannot be measured due to turbulent mixing.

5. Summary

Convection inside an EM-levitated Zr sample in microgravity was predicted using the MHD model which had been developed and experimentally validated in the previous research. The maximum convection velocity and the corresponding Reynolds number were predicted under possible combinations of the positioner and heater control voltages at various temperatures. Based on the predicted convection status, the feasibility of the measurement of some thermophysical properties sensitive to convection, such as viscosity and thermal conductivity was evaluated. For the case of viscosity, the positioner control voltage must be kept below 6 V in order not to induce turbulence. Meanwhile, under the planned range of temperature (1923 – 2193 K) for the modulation calorimetry, the flow will always be turbulent. With turbulence, heat capacity can be measured effectively with help of turbulent mixing, however, thermal conductivity cannot be measured because the generated heat in the skin depth area will be transferred mainly by convection rather than conduction.

Acknowledgement

This research has been supported by NASA under grant NNX10AR71G.

References

1) J. Lee, D.M. Matson, S. Binder, M. Kolbe, D. Herlach and R.W. Hyers: Metall. Mater. Trans., **45B** (2014) 1018.
2) J. Lee, X. Xiao, D.M. Matson and R.W. Hyers: TMS2013 Suppl. Proc., (2013) DOI: 10.1002/9781118663547.ch58.
3) R.W. Hyers, G. Trapaga and B. Abedian: Metall. Mater. Trans., **34B** (2003) 29.
4) J. Lee, X. Xiao, D.M. Matson and R.W. Hyers: Metall. Mater. Trans., (2014) DOI: 10.1007/s11663-014-0178-9. .
5) R.C. Bradshaw, M.E. Warren, J.R. Rogers, T.J. Rathz, A.K. Gangopadhyay, K.F. Kelton and R.W. Hyers: Ann. N.Y. Acad. Sci., **1077** (2006) 63.
6) H.-J. Fecht and L. Johnson: Rev. Sci. Instrum., **62** (1991) 1299.
7) R.K. Wunderlich, H.-J. Fecht and W. R.: Appl. Phys. Lett., **62** (1993) 3111.
8) R.K. Wunderlich, D.S. Lee, W.L. Johnson and H.-J. Fecht: Phys. Rev. B, **55** (1997) 26.
9) S. Berry, R.W. Hyers, B. Abedian and L.M. Racz: Metall. Mater. Trans., **31B** (2000) 171.